Available online at www.sciencedirect.com
SCIENCE DIRECT®
ELSEVIER
Journal of Magnetism and Magnetic Materials 288 (2005) 79–83
Journal of magnetism and magnetic materials
www.elsevier.com/locate/jmmm

Magnetic and thermal properties of Ni–Mn–Ga shape memory alloy with Martensitic transition near room temperature

F.Q. Zhu[a,*], F.Y. Yang[a], C.L. Chien[a], L. Ritchie[b], G. Xiao[b], G.H. Wu[c]

[a]*Department of Physics and Astronomy, The Johns Hopkins University, Baltimore, MD 21218, USA*
[b]*Physics Department, Brown University, Providence, RI 02912, USA*
[c]*Institute of Physics, Chinese Academy of Science, Beijing, China*

Received 11 February 2004; received in revised form 19 August 2004
Available online 25 September 2004

Abstract

We have studied the magnetic properties of an off-stoichiometric Heusler shape memory alloy $Ni_{51.9}Mn_{23.2}Ga_{24.9}$ with near room temperature martensitic transition at 306 K. The temperature dependence of magnetization revealed a thermal hysteresis and a ~10% decrease in spontaneous magnetization across the martensitic transition. In-situ X-ray diffraction measurements at different temperatures revealed a negative shape strain of 4.8%. Heat absorptions measurements indicated that the martensitic structural transition may take place in multiple steps.

PACS: 81.30.Kf; 61.10.Nz; 65.50.Ba; 75.50.-s

Keywords: Shape memory alloy; Heusler alloy; Spontaneous magnetization; Martensitic transition

1. Introduction

Ferromagnetic shape memory alloys (FSMAs) combine the properties of ferromagnetism with those of a diffusionless, reversible martensitic transition. In recent years, much attention has been focused on Ni_2MnGa and its off-stoichiometric alloys [1–7]. Because its martensitic phase exhibits an unusually large magnetostriction, Ni_2MnGa has potential applications as a magnetically controlled actuator material. A magnetic field induced strain (MFIS) of up to 6% has been reported [5,8]. However, the usefulness of Ni_2MnGa for applications is limited by its low martensitic transition temperature (T_M near 200 K) and low Curie temperature ($T_C = 376$ K).

By varying the Ni–Mn–Ga composition, one can change the transition temperatures of the resulting alloy. Fig. 1 is the phase diagram of $Ni_{2+x}Mn_{1-x}Ga$ [9]. At high temperature, the

*Corresponding author. Tel.: +1-410-516-8701; fax: +1-410-516-7239
E-mail address: qzhu@pha.jhu.edu (F.Q. Zhu).

0304-8853/$ - see front matter © 2004 Elsevier B.V. All rights reserved.
doi:10.1016/j.jmmm.2004.08.025

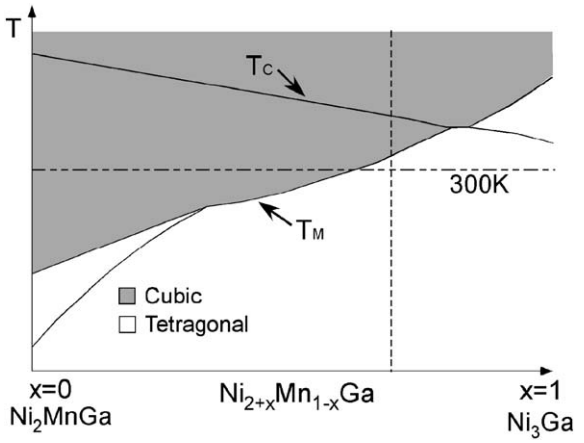

Fig. 1. Phase diagram for $Ni_{2+x}Mn_{1-x}Ga$. The labeled lines correspond to the structural (T_M) and ferromagnetic (T_C) phase transitions. The cubic (austenitic) phases are shaded, while the tetragonal (martensitic) phases are unshaded. The vertical dashed line, which is approximated using our calculated values for T_M and T_C, is representative of our sample composition.

Ni–Mn–Ga system has a cubic structure (austenite), represented by the shaded area. The unshaded area corresponds to the tetragonal structure (martensite) which the alloy assumes below T_M. The phase diagram illustrates that as Ni composition x increases, T_M increases and T_C decreases. T_M and T_C approach one another and become equal at some critical Ni concentration. The phase diagram suggests that it is possible to engineer a Ni–Mn–Ga alloy with T_M near room temperature, but still less than T_C. Our sample composition, $Ni_{51.9}Mn_{23.2}Ga_{24.9}$, was chosen with this goal in mind. The fabrication process has been published elsewhere [10]. This work focuses on the temperature dependence of magnetic properties of this sample. A ~10% decrease in spontaneous magnetization across the martensitic transition has been observed. More interestingly, the transition may take place in multiple steps as revealed by heat absorption measurements.

2. Experimental details

All of our magnetic measurements were made using a Quantum Design SQUID magnetometer in a temperature range between 5 and 400 K and a maximum field of 5 T. Sample was mounted inside a quartz tube whose low thermal expansion coefficient reduces sample position change during thermal sweeping. X-ray diffraction (XRD) scans were performed on a Philips 3720 XRD system. Modification was made on the sample stage to accommodate XRD at various temperatures. Perkin-Elmer DSC2 differential scanning calorimeter (DSC) was used to monitor heat absorption during the transitions. Samples were sealed in a standard Cu cup and measured together with another same sized empty cup to remove the contribution from the cup itself.

3. Results and discussion

To estimate T_C and determine the structural transition temperatures, we measured the temperature dependence of magnetization between 5 and 400 K in a small magnetic field of 0.1 mT (see Fig. 2 inset). Measurements were carried out using both zero field cooling (ZFC) and field cooling (FC) processes. The measurements indicate a Curie temperature near 364 K, above which the magnetization vanishes for both processes. We can also clearly see the sharp phase transitions at 306 and 315 K, which correspond to the martensitic and the reverse martensitic transition temperatures, respectively. At 0.1 mT, which is far less than the saturation field of either phase, the measured magnetization of the austenitic (high-temperature) phase is larger than that of the martensitic (low-temperature) phase. The smaller magnetization of the martensite implies that it must have a larger anisotropy. The martensite's comparatively flat magnetization curve is also an evidence of a large anisotropy. Magnetically, the austenite is softer and more easily saturated than the martensite. Finally, we note that repetition of the low-field magnetic measurements yielded identical results. This reproducibility of the structural transition, even after repeated thermal cycling, indicates a strong potential for applications.

At higher magnetic fields, the anisotropy energy becomes less competitive with the magnetic

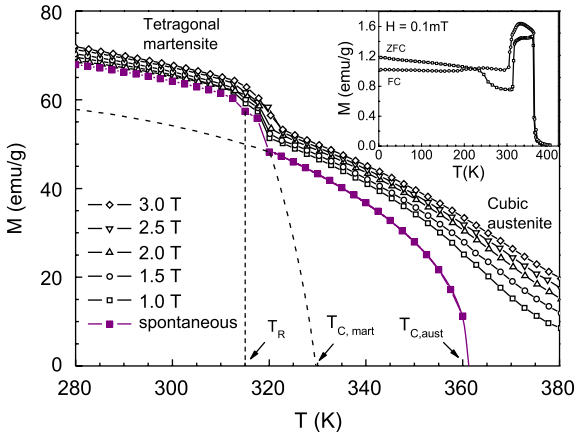

Fig. 2. Temperature dependence of magnetization of $Ni_{51.9}Mn_{23.2}Ga_{24.9}$ at a series of fields greater than saturation. Solid squares represent the spontaneous magnetization as calculated using the Arrott plot method. The inset shows M vs. T for a very small (unsaturated) field of 0.1 mT. The sharp transitions of the FC (field cooled) and ZFC (zero field cooled) curves indicate the martensitic and reverse martensitic transitions, respectively.

energy. As the magnetic field is increased beyond 0.2 T, the magnetization of the martensite surpasses that of the austenite. Fig. 2 shows a series of M vs. T curves measured using the ZFC method at fixed fields of 1 T or greater. At these fields, which are larger than the saturation fields of both phases, the anisotropy energy is negligible. As with a normal ferromagnet, the magnetization decreases as temperature increases. However, our measurements indicate a sharp decrease in magnetization at the structural transition temperature. The decrease is significant, amounting to a nearly 10% reduction in magnetization between 314 and 319 K. To our knowledge, this phenomenon has not been previously observed.

To understand this better, we used our high-field magnetization data to generate a plot of spontaneous magnetization (M_0) as a function of temperature. The resulting M_0 vs. T curve, shown as solid squares in Fig. 2, was extrapolated from our data using the Arrott plot method [11]. Spontaneous magnetization is 81.3 emu/g at 5 K, and decreases to 0 at $T_C = 361.26$ K. The M_0 vs. T curve in Fig. 2 can be seen as the combination of two single-phase M_0 vs. T curves: one corresponding to the martensitic phase, and the other corresponding to the austenitic phase. For a given T, the martensite and austenite have different M_0, except at 319 K transition, where the two single-phase curves must intersect. The dashed line in Fig. 2 corresponds to the single-phase curve for the austenitic phase. Below the transition temperature, the austenitic phase has a lower M_0. More specifically, at 5 K, the martensite has $M_{0,\mathrm{mart}} = 81.3$ emu/g, while the austenite has $M_{0,\mathrm{aust}} \approx 70$ emu/g. Although the data does not allow us to accurately extrapolate a single-phase curve for the martensite, $T_{C,\mathrm{mart}}$ is most likely lower than $T_{C,\mathrm{aust}}$.

Hysteresis loops were measured at a series of temperatures from 5 to 400 K. Fig. 3 shows representative loops at 5, 300, and 325 K. At 5 and 300 K, the saturation field is about 1 T, while at 325 K it is only 0.2 T. This dramatic change in saturation field is attributable to the structural transition at 315 K. The inset of Fig. 3 is a plot of coercivity values for temperatures near the transition. The data of the inset shows how the alloy transitions from the harder martensite to the softer austenite. Below 315 K, the coercivity is large and decreases rapidly with increasing temperature; above 315 K, the coercivity is smaller and

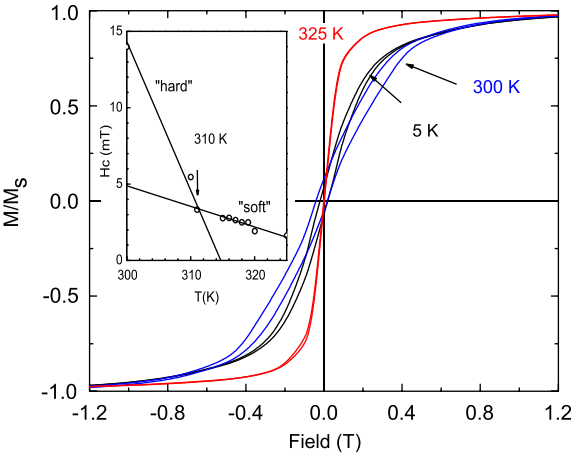

Fig. 3. Representative hysteresis loops of $Ni_{51.9}Mn_{23.2}Ga_{24.9}$ for the martensitic (5 and 300 K) and the austenitic (325 K) phases. Temperature dependence of the coercivity is plotted in the inset. Solid lines are linear fits to the coercivity data for the two phases.

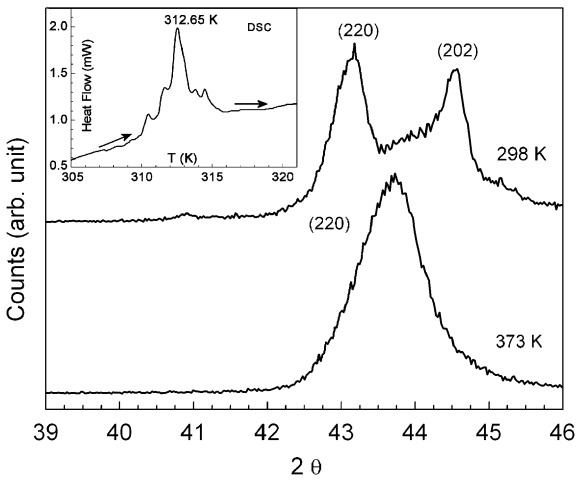

Fig. 4. X-ray diffraction scans of the martensitic and austenitic phases of $Ni_{51.9}Mn_{23.2}Ga_{24.9}$. The tetragonal structure of the martensitic phase causes the (2 2 0) and (2 0 2) peaks to become distinct. The inset is a plot of heat flow during the heating process. The small satellite peaks which flank the central peak indicate that the structural transition takes place in multiple steps.

decreases slowly with increasing temperature. The solid lines are linear fits to the coercivity data for the two regions.

X-ray diffractions were measured to determine the shape strain associated with the structural transition. Two representative isothermal XRD scans, one at room temperature (298 K) and another one at 373 K, are shown in Fig. 4. At 373 K, the alloy is in the austenitic phase and has a cubic structure. The (2 2 0) peak at 43.7° indicates a cubic lattice constant of 5.852 Å. At 298 K, the alloy is in the martensitic phase and has a tetragonal structure. For this structure, the (2 2 0) and (2 0 2) peaks are distinct. From the XRD peaks at 43.1° and 44.5°, we determine the lattice constants: $a = b = 5.928$ Å and $c = 5.582$ Å, which are very close to those reported by others [12]. Finally, using $\Delta c/c$ as the definition of shape strain, we find a very large shape strain of −4.8%.

A phase transition is usually accompanied by a heat transfer, so monitoring the heat flow during the heating or cooling process can give us an accurate indication of the phase transition temperature. A differential scanning calorimeter was used to measure the heat flow of a small chunk of alloy (mass is 12.86 mg) as the temperature was increased from 298 to 373 K at 5 K/min (see Fig. 4 inset). The resulting heat flow data reveals a prominent peak at 312.65 K, flanked by several small satellite peaks. The peak at 312.65 K clearly corresponds to the reverse martensitic phase transition, which we know occurs near 315 K in a small magnetic field of 0.1 mT. The existence of the satellite peaks indicate that the alloy transition from tetragonal structure to cubic structure takes place in multiple steps. The identification of these steps and how they correspond to the structure of the alloy is still under investigation. Heat flow measurements were also performed for temperatures near T_C, no discernable peaks in the heat flow data were found, so we conclude that the heat transfer associated with the ferromagnetic transition is negligible.

4. Conclusion

In summary, we have successfully fabricated the ferromagnetic shape memory alloy $Ni_{51.9}Mn_{23.2}Ga_{24.9}$. Magnetic measurements indicate that our alloy has $T_C = 361.26$ K, $T_M = 306$ K, and $T_R = 315$ K. The structural transition temperatures are very close to room temperature, making this alloy potentially useful for application. In the martensitic phase, the alloy has a tetragonal structure, and is characterized by large anisotropy and coercivity. The coercivity is also more strongly temperature dependent in the martensitic phase than in the austenitic phase. In the austenitic phase, the alloy has a cubic structure, a smaller anisotropy, and a smaller, less temperature dependent, coercivity. As a result of the transition from a magnetically hard martensitic phase to a softer austenitic phase, the spontaneous magnetization exhibits a sharp drop (~10%) in the vicinity of the structural transition temperature. From XRD measurements, we determine a large negative shape strain of 4.8% associated with the martensitic transition. Finally, heat absorption measurements indicate that the martensitic transition may take place in multiple steps, with the major structural transition occurring at 312.65 K in zero field.

Acknowledgement

This work was supported by NSF Grant nos. DMR01-01814 and DMR00-80031.

References

[1] A.N. Vasil'ev, S.A. Klestov, R.Z. Levitin, V.V. Snegirev, V.V. Kokorin, V.A. Chernenko, JETP Lett. 82 (1996) 524.
[2] K. Ullakko, J.K. Huang, C. Kantner, V.V. Kokorin, R.C. O'Handley, Appl. Phys. Lett. 69 (1996) 1966.
[3] R.C. O'Handley, J. Appl. Phys. 83 (1998) 3263.
[4] R. Tickle, R.D. James, T. Shield, M. Wuttig, V.V. Kokorin, IEEE Trans. Magn 35 (5) (1999) 4301; R.D. James, M. Wuttig, Phil. Mag. Lett. A 77 (1998) 1273.
[5] S.J. Murray, M. Marioni, P.G. Tello, S.M. Allen, R.C. O'Handley, J. Magn. Magn. Mater. 226–230 (2001) 945; S.J. Murray, M. Marioni, S.M. Allen, R.C. O'Handley, Appl. Phys. Lett. 77 (2000) 886.
[6] W.H. Wang, G.H. Wu, J.L. Chen, S.X. Gao, W.S. Zhan, G.H. Wen, X.X. Zhang, Appl. Phys. Lett. 79 (2001) 1148; G.H. Wu, C.H. Yu, L.Q. Meng, J.L. Chen, F.M. Yang, S.R. Qi, W.S. Zhan, Z. Wang, Y.F. Zheng, L.C. Zhao, Appl. Phys. Lett. 75 (1999) 2990.
[7] M. Wuttig, L. Liu, K. Tsuchiya, R.D. James, J. Appl. Phys. 87 (2000) 4707.
[8] A.A. Likhachev, K. Ullakko, Phys. Lett. A 275 (2000) 142.
[9] A.D. Bozhko, A.N. Vasil'ev, V.V. Khovailo, V.D. Buchel'nikov, I.E. Dikshtein, S.M. Seletskii, V.G. Shavrov, JETP Lett. 67 (1998) 227.
[10] W.H. Wang, G.H. Wu, J.L. Chen, C.H. Yu, S.X. Gao, W.S. Zhan, Z. Wang, Y.F. Zhang, L.C. Zhao, Appl. Phys. Lett. 77 (2000) 3245.
[11] A. Arrott, J.E. Noakes, Phys. Rev. Lett. 19 (1967) 786.
[12] Y. Ma, S. Awaji, K. Watanabe, M. Natsumoto, N. Kobayashi, Solid State Commun. 113 (2000) 671.